ORIGINAL ARTICLE

http://dx.doi.org/10.4046/trd.2014.77.3.116
ISSN: 1738-3536(Print)/2005-6184(Online) • Tuberc Respir Dis 2014;77:116-123

TRD
Tuberculosis and Respiratory Diseases

Tracking Intravenous Adipose-Derived Mesenchymal Stem Cells in a Model of Elastase-Induced Emphysema

You-Sun Kim, Ph.D.[1,2], Ji-Young Kim, M.S.[1], Dong-Myung Shin, Ph.D.[3], Jin Won Huh, Ph.D.[4], Sei Won Lee, Ph.D.[4] and Yeon-Mok Oh, M.D., Ph.D.[1,2,4]

[1]Asan Institute for Life Science, [2]University of Ulsan College of Medicine, [3]Department of Biomedical Sciences, Asan Medical Center, University of Ulsan College of Medicine, [4]Department of Pulmonary and Critical Care Medicine, Asthma Center, Clinical Research Center for Chronic Obstructive Airway Diseases, Asan Medical Center, Seoul, Korea

Background: Mesenchymal stem cells (MSCs) obtained from bone marrow or adipose tissue can successfully repair emphysematous animal lungs, which is a characteristic of chronic obstructive pulmonary disease. Here, we describe the cellular distribution of MSCs that were intravenously injected into mice with elastase-induced emphysema. The distributions were also compared to the distributions in control mice without emphysema.
Methods: We used fluorescence optical imaging with quantum dots (QDs) to track intravenously injected MSCs. In addition, we used a human Alu sequence-based real-time polymerase chain reaction method to assess the lungs, liver, kidney, and spleen in mice with elastase-induced emphysema and control mice at 1, 4, 24, 72, and 168 hours after MSCs injection.
Results: The injected MSCs were detected with QD fluorescence at 1- and 4-hour postinjection, and the human Alu sequence was detected at 1-, 4- and 24-hour postinjection in control mice (lungs only). Injected MSCs remained more in mice with elastase-induced emphysema at 1, 4, and 24 hours after MSCs injection than the control lungs without emphysema.
Conclusion: In conclusion, our results show that injected MSCs were observed at 1 and 4 hours post injection and more MSCs remain in lungs with emphysema.

Keywords: Mesenchymal Stromal Cells; Emphysema; Cell Tracking; Injections, Intravenous

Address for correspondence: Yeon-Mok Oh, M.D., Ph.D.
Department of Pulmonary and Critical Care Medicine, Asthma Center, Clinical Research Center for Chronic Obstructive Airway Diseases, Asan Medical Center, 88 Olympic-ro 43-gil, Songpa-gu, Seoul 138-736, Korea
Phone: 82-2-3010-3136, **Fax:** 82-2-3010-4650
E-mail: ymoh55@amc.seoul.kr
Received: May 13, 2014
Revised: Jun. 20, 2014
Accepted: Jun. 24, 2014

Introduction

Stem cell-based cell therapy is relatively successful, demonstrating beneficial therapeutic effects across a wide range of disease such as heart disease, bone disease, cancer, hepatic disease, and lung disease[1-8]. Some preclinical trials report the therapeutic effects of using stem cells to treat chronic obstructive pulmonary disease (COPD), which is characterized by emphysema and chronic bronchitis[9-11]. Our recent research shows that bone marrow-derived mesenchymal stem cells (MSCs) are able to repair cigarette smoke-induced emphysema[9]. Other research also report that MSCs from bone marrow and adipose tissue demonstrate therapeutic effects against cigarette smoke- and elastase-induced emphysema[11-14].

However, the role of engraftment in the mechanism of ac-

tion of adult stem cells is controversial because engraftment rates of adults stem cells are low in recent studies[15,16]. In our previous study, only a few stem cells were observed from 1 day through 1month after intravenous injection[9]. Though many cells initially localize in the lungs as the major capillary bed encountered after systemic administration, the overall donor cell retention is minimal. It is important to know the distribution of systemically (intravenously) injected stem cells that need to be administered to COPD patients in clinical trials. Optical imaging demonstrates several advantages for tracking the distribution of injected cells: it is rapid, nontoxic, and provides the visible whole-body distribution. Detecting fluorescence is a general analytical method that uses a computer-controlled display detector. Quantum dot (QD) labeling kit is a commercially available for fluorescent labeling of cells and has strong intense, stable fluorescence that can be visible through several generations[17,18].

Another method for tracking the distribution of injected human cells into mice is Alu sequencing. Alu sequences are present in 500,000–1,000,000 copies in the human genome and are observed primate specific[19,20]. Previous studies developed Alu-based real-time polymerase chain reaction (PCR) methods for quantifying human DNA in mixed samples obtained from various species[21,22].

In our present study, we evaluate the distribution of intravenously injected MSCs by detecting fluorescence-labeled cells and the human Alu sequence in mice lung *ex vivo*. We also observed the distribution of intravenously injected MSCs in elastase-induced emphysematous mice.

Materials and Methods

1. Mice

C57BL/6 mice were purchased from Orient Bio (Seongnam, Korea). Mice were housed in a specific pathogen-free facility. All animal experiments were approved by the Institutional Animal Care and Use Committee of Asan Medical Center (Korea).

2. Induction of pulmonary emphysema and cell transplantation

To generate elastase induced model, 6-week-old female C57BL/6J mice were intratracheally instilled with porcine pancreatic elastase (Sigma-Aldrich, St. Louis, MO, USA). Each animal was intratracheally injected 0.4 U of elastase at day 0. The mice were intravenously injected with 5×10^5 of MSCs on day 7.

3. MSC culture and labeling

Human adipose-derived MSCs were purchased from Invitrogen (Carlsbad, CA, USA). MSCs were cultured in Mesen PRO RS Basal Medium supplemented with Mesen PRO RS growth supplement (Invitrogen) and incubated at 37°C in a 5% CO_2 atmosphere. Cells were used after 2–5 passages. MSCs were labeled using the QDs (Q-Tracker 800) Cell Labeling Kit (Invitrogen). MSCs (1×10^6) were suspended with 200 μL of complete growth medium and labeled with 10 nM of QDs labeling solution. After 60 minutes, labeled cells with QDs were washed twice with complete growth medium.

4. *Ex vivo* fluorescent imaging of QD-labeled MSCs

In total, 5×10^5 QDs 800-labeled MSCs were placed in 100 μL saline and injected into the mice through the tail vain. Mice were sacrificed after 1, 4, 24, 72, and 168 hours, and images of the major organs (e.g., lung, liver, and spleen kidneys) were taken using the IVIS Spectrum Pre-clinical In vivo Imaging System (PerkimElmer, Waltham, MA, USA).

5. DNA extraction and quantitative PCR (qPCR) analysis

Standard genomic DNA samples were prepared using human adipose-derived MSCs (Invitrogen). Genomic DNA samples were isolated from murine organs, including the lungs, liver, spleen and kidneys, using a genomic DNA extraction kit (Qiagen, Duesseldorf, Germany).

6. Primer design and PCR amplification

The primers for Alu were 5′-CGAGGCGGGTGGATCATGAGGT-3′ and 5′-TCTGTCGCCCAGGCCGGACT-3′. To perform the Light Cycler reaction, a master mix of the following reaction components was prepared to the indicated end-concentration: 10 μL of 2× SYBR green buffer, 1 μL forward primer (10 pM), 1 μL reverse primer (10 pM), and 8 μL DNA template (10 ng). The following LightCycler experimental protocol was used: initial denaturation for 12 minutes at 95°C, followed by 40 amplification cycles of 95°C for 15 seconds and 70°C for 1 minute to anneal and extend, respectively. Quantitative PCR experiments were performed using LightCycler 480 Software (Roche Diagnostics, Basel, Switzerland).

7. Data analysis

Statistical analyses were performed using the Graphpad Prism ver. 5 (GraphPad software, La Jolla, CA, USA). The Mann-Whitney test was used to compare both groups, and statistical significance was set at $p<0.05$.

Results

1. MSC distribution after intravenous injection

To observe the intravenously injected MSCs, we injected

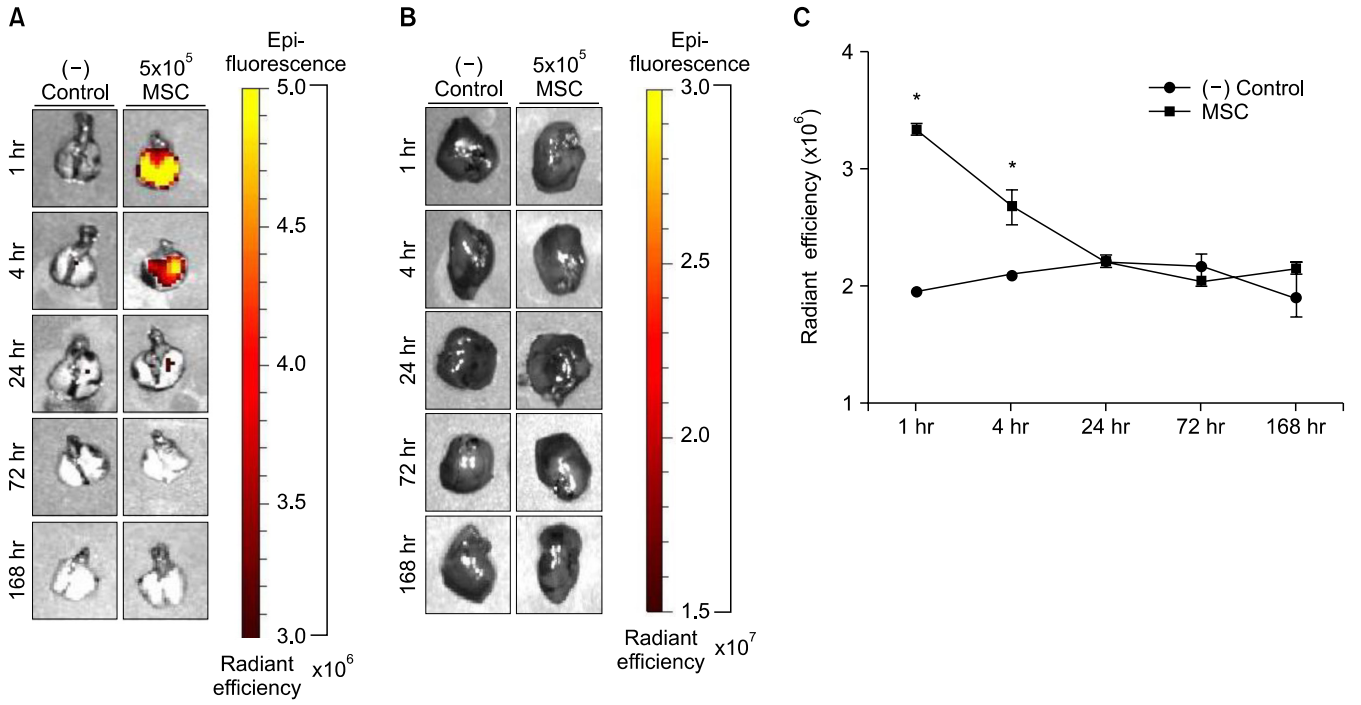

Figure 1. *Ex vivo* fluorescence imaging and intensity analysis various time after intravenously quantum dots (QDs)-labeled mesenchymal stem cell (MSC) injection. (A) The *ex vivo* fluorescence images of the lung from control mice or intravenously QDs labeled in MSC-injected mice. (B) The *ex vivo* fluorescence images of the liver from control mice or intravenously QDs labeled in MSC-injected mice. Representative images are shown (n=3). (C) Radiant efficiency of the lung from control mice or MSC-injected mice. The data had a significant difference (*p<0.05) between the control group and the MSC-injected group.

5×10^5 MSCs that had been labeled with 10 nM QDs. After injection, fluorescent signaling was detected in the lungs in 4 hours, but this signal gradually decreased (Figure 1A). The liver did not demonstrate any fluorescent signals (Figure 1B). There were no fluorescent signals in the kidneys or spleen in MSC-injected mice (data not shown). To determine fluorescent intensity, regions that contained only 1 organ were selected and region of interest (ROI) values were obtained. The intensity of the fluorescent signals in the MSC-injected mice was only detected in the lungs at 4 hours after intravenous injection (Figure 1C).

2. Quantitative PCR analysis using human Alu sequences

To assess the optical imaging data and quantify the relative amount of transplanted MSCs, we prepared genomic DNA obtained from the organs (including the lungs, liver, kidneys, and spleen) of MSC-injected and non-injected mice and performed quantitative PCR using human-specific Alu sequence primers. A previous study developed an assay that detects samples in real-time using human Alu-specific PCR and SYBR Green I. To validate assay using human Alu-specific sequence, the regression r^2 value was calculated by performing quantitative PCR using 10 ng of genomic DNA from 10, 10^2, 10^3, 10^4, 10^5, and 10^6 numbers of MSCs (Figure 2A). The calculated r^2 value was 0.998, and this was used as the standard curve to determine the number of transplanted MSCs. The number of MSCs in the lungs was about 3,500 after 1-hour postinjection and gradually decreased with time (Figure 2B). MSCs were undetectable at 72-hour postinjection and were undetectable in the liver at all times (Figure 2C). In addition, no MSCs were detectable in the kidneys or spleen (data not shown).

3. MSC distribution after intravenous injection into elastase-induced emphysematous mice

To evaluate the distribution of intravenously injected MSCs in elastase-induced emphysema mice, the animals were intratracheally injected with 0.4 U porcine pancreas-derived elastase and intravenously injected with 5×10^5 QD-labeled MSCs at 7 days after elastase injection. More fluorescent signals were detected in the lungs of elastase-injected mice than non-elastase-injected mice (Figure 3A). MSCs in the lungs of elastase-induced emphysematous mice—but not non-elastase-injected mice—were detectable at 24 hours after injection. ROI analysis showed that larger amounts of MSCs had accumulated in the lungs of emphysematous mice in comparison with the lungs in non-elastase-injected mice at every documented time point

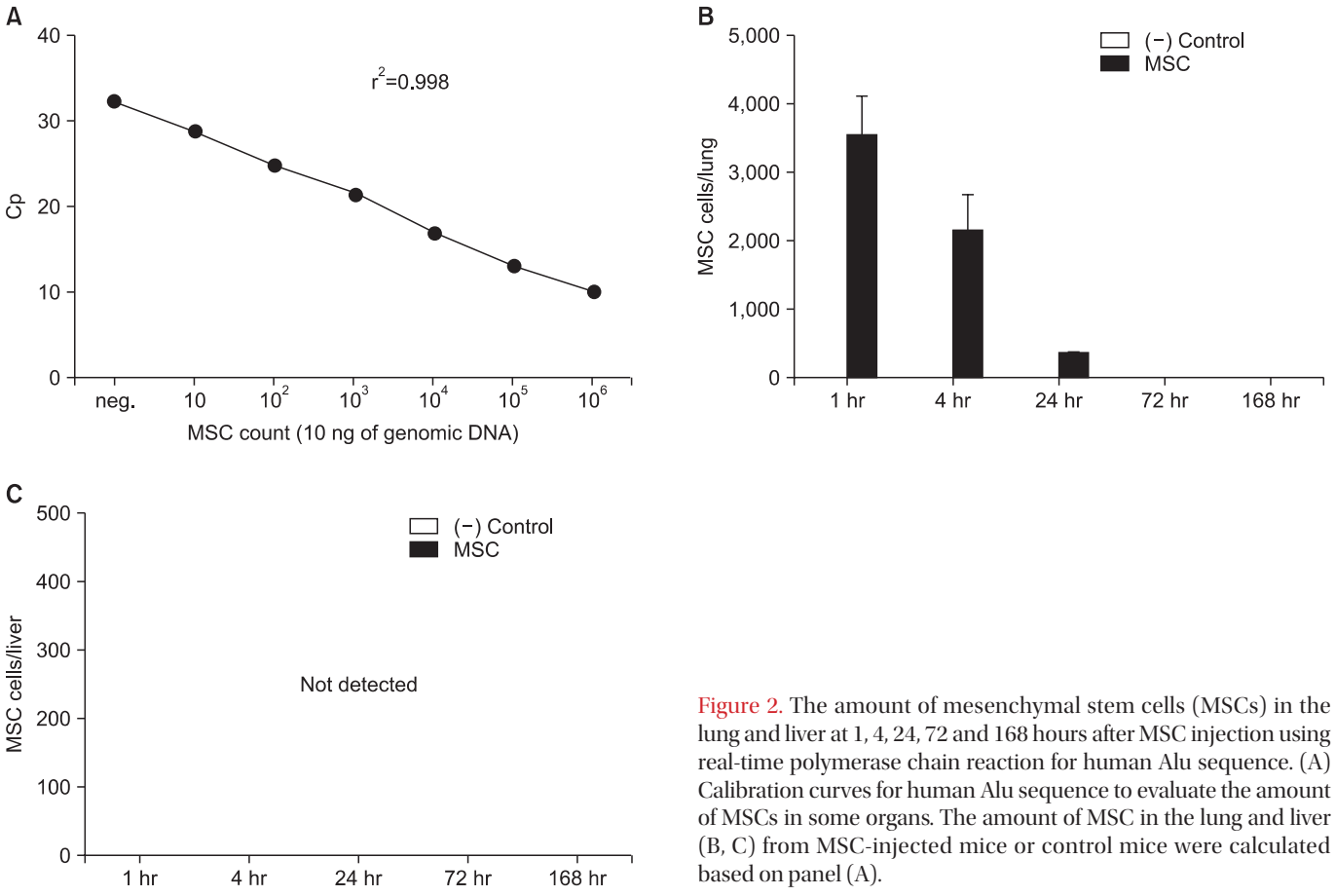

Figure 2. The amount of mesenchymal stem cells (MSCs) in the lung and liver at 1, 4, 24, 72 and 168 hours after MSC injection using real-time polymerase chain reaction for human Alu sequence. (A) Calibration curves for human Alu sequence to evaluate the amount of MSCs in some organs. The amount of MSC in the lung and liver (B, C) from MSC-injected mice or control mice were calculated based on panel (A).

(Figure 3B). The intravenously injected MSCs disappeared from the lungs of the emphysematous mice and control mice at 72 hours (Figure 4). There were no fluorescent signals in the liver, kidneys, or spleen in either the emphysematous or non-elastase-injected mice (Figure 5). MSCs were maintained for longer periods of time in emphysematous mice.

Discussion

We here observed intravenously injected MSCs using optical imaging and Alu-based real-time PCR and compared MSCs distributions between emphysematous and control mice. QD-labeled MSCs were detected at 4-hour postintravenous injection in the lungs. No QD-labeled MSCs were observed in any other major organ, including the liver, kidneys, and spleen. These relative quantification methods in murine organs use human Alu-and xenograft-based real-time PCR. We were able to detect 10–10^6 MSCs per 10 ng genomic DNA. Intravenously injected MSCs were observed at 24 hours, but gradually decreased with time. Next, we intravenously injected MSCs into structure destructed emphysematous lung (on day 7 after elastase injection) because we focused on basic data to obtain for clinical application. Emphysematous lungs maintained more MSCs for longer periods of time in comparison with controls through 24 hours after injection.

The systemic injection of MSCs is relatively easy in clinical settings. Easy application allows intravenously injected MSCs to demonstrate high levels of initial accumulation for the treatment of pulmonary diseases. Our previous study has shown that that treatment with bone marrow cells (BMCs) can repair cigarette smoke-induced emphysema[9,23]. Moreover, intravenously injected BMCs from male animals are rarely detected in female recipients after 1 month[9,14]. ^{111}In-oxine-labeled MSCs that were co-labeled with ferumoxides-poly-L-lysine were detected using combination single-photon emission computed tomography (SPECT), X-ray computed tomography (SPECT/CT), and magnetic resonance imaging in an animal model of acute myocardial infarction[24]. Enhanced green fluorescent protein (EGFP)-labeled MSCs were also tracked in a model of liver injury[25]. We used QDs with near-infrared region (NIR) emission to label MSCs. QDs are characterized by the deep penetration of excitation and emission light in the NIR region and low autogenetic fluorescence. QD-labeled stem cells are not affected in terms of viability, proliferation, or differentiation in comparison with non-labeled stem cells[26]. In our

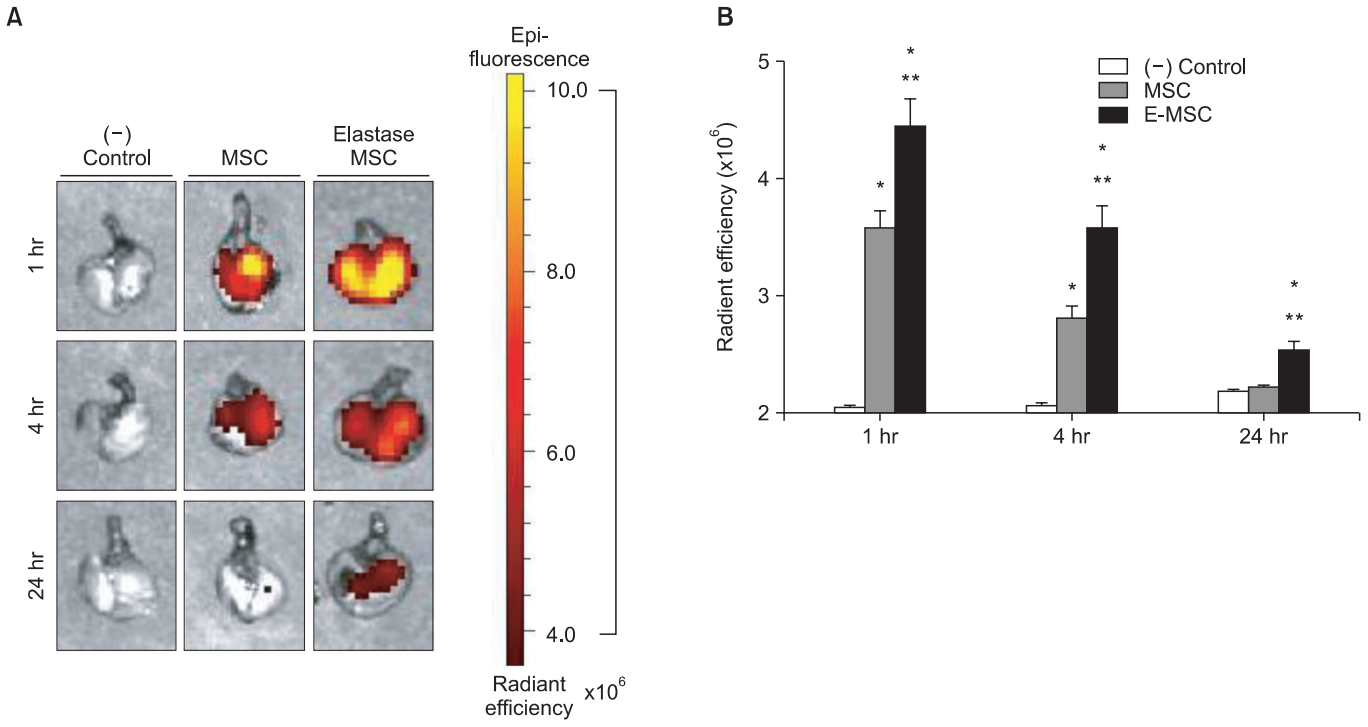

Figure 3. *Ex vivo* fluorescence imaging and intensity 1, 4, and 24 hours after intravenously quantum dots (QDs)-labeled mesenchymal stem cell (MSC) injection with elastase-induced emphysema. (A) The *ex vivo* fluorescence images of the lung from control mice or intravenously QDs-labeled MSC-injected mice with or without elastase-induced emphysema. Representative images are shown (n=7). (B) Radiant efficiency of the lung from control mice or MSC-injected mice with or without elastase-induced emphysema. The data had a significant difference (*p<0.05) between the control group and the MSC-injected group; **p<0.05 between MSC injected with and without elastase-induced emphysema group.

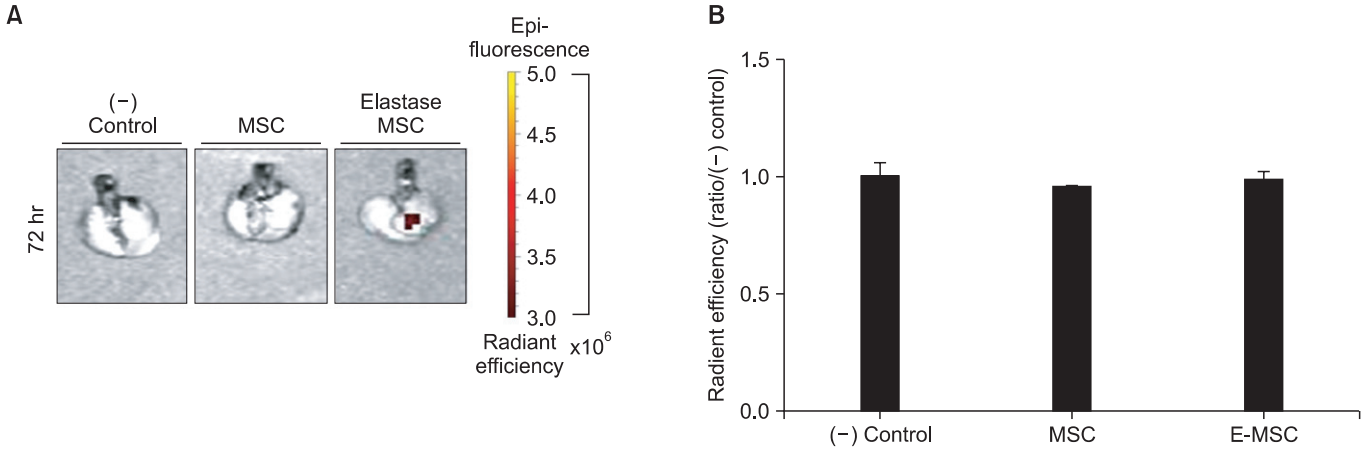

Figure 4. *Ex vivo* fluorescence imaging 72 hours after intravenously quantum dots (QDs)-labeled mesenchymal stem cell (MSC) injection with elastase-induced emphysema. (A) The *ex vivo* fluorescence images of the lung from control mice or intravenously QDs-labeled MSC-injected mice with or without elastase-induced emphysema. Representative images are shown (n=7). (B) Radiant efficiency of the lung from control mice or MSC-injected mice with or without elastase-induced emphysema. The data did not have a significant difference.

current study, we first observed intravenously injected QD-labeled MSCs at various times in elastase-induced emphysema model.

The detection for MSCs using molecular levels such as DNA and RNA were tired with stem cell from EGFP transgenic mice using techniques of qPCR for EGFP gene[27]. This assay quan-

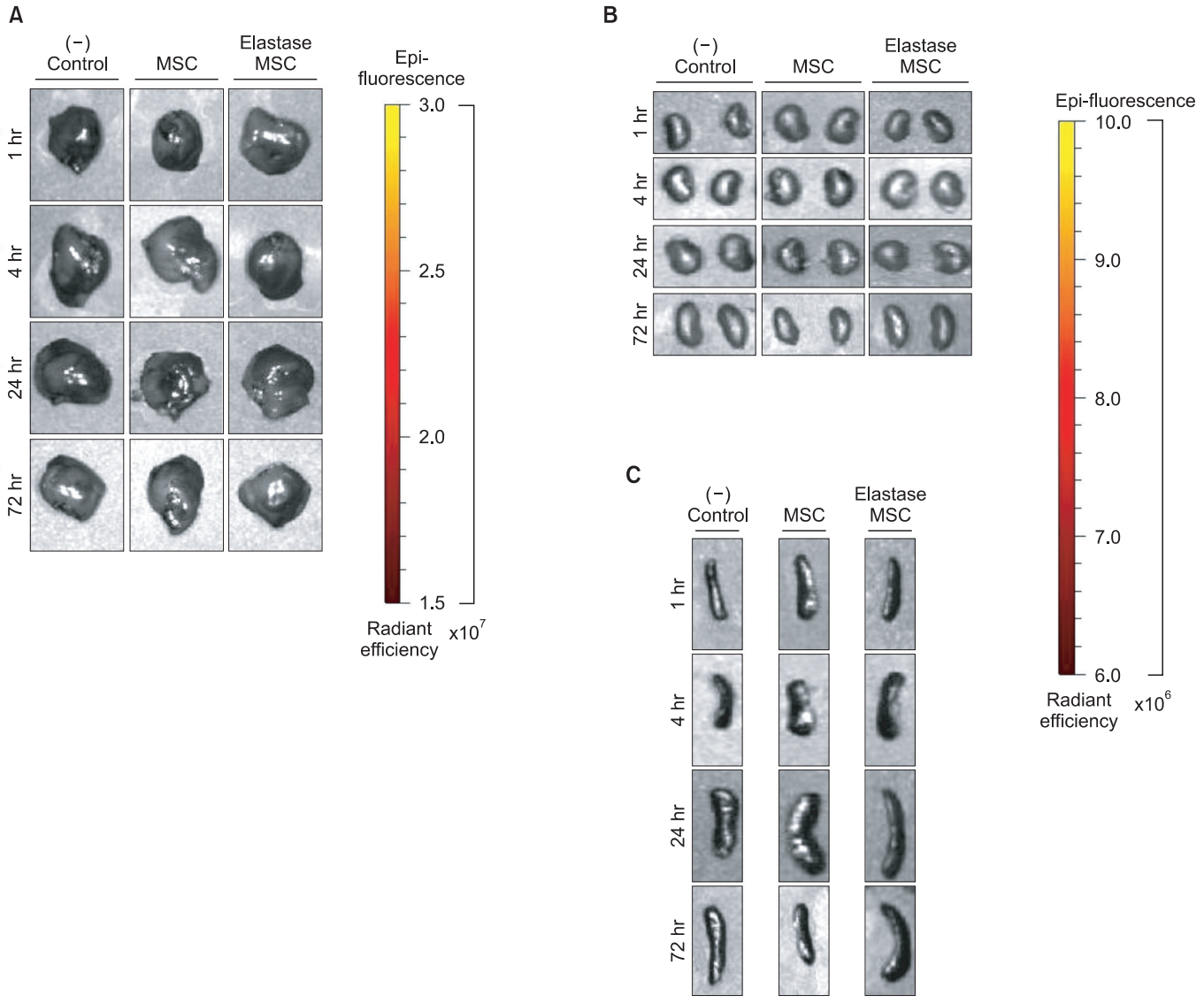

Figure 5. *Ex vivo* fluorescence imaging 1, 4, 24, and 72 hours after intravenously quantum dots (QDs)-labeled mesenchymal stem cell (MSC) injection with elastase-induced emphysema. The *ex vivo* fluorescence images of the liver, kidney or spleen (A–C) from control mice or intravenously QDs-labeled MSC-injected mice with or without elastase-induced emphysema. Representative images are shown (n=7).

tifies the relative number of EGFP optimized by beta-actin genes, but low cell numbers, such as 10 $EGFP^+$ cells per 10^5 total cells, were undetectable. The Alu-based quantification of human DNA requires real-time PCR and human Alu-specific primers[21,22]. We used Alu-based real-time PCR to relatively quantify some organs, such as the lungs, liver, and kidneys, and we successfully observed about 3,500 numbers of MSCs in the lungs without specifically genetically manipulating the mice, including EGFP transgenic mice.

Stem cell homing and engrafting to injury sites has been performed previously in some disease models, including those for traumatic brain injury, liver injury, and cardiac and brain injuries[24,25,28]. The recruitment of stem cells to the injury site relies on well-known mechanisms that release various chemokines and cytokines[29]. Representative signals include stromal-derived factor-1 (SDF-1) and the CXCR4 axis at the injury site and stem cell surface, respectively[29-31]. Although there are no data indicating that SDF-1 or the CXCR4 axis affect stem cell homing and mobilization into emphysematous lungs in present our results, the axis is related to the recruitment of stem cells to the injury sites of other diseases, such as inflammatory bowel disease and myocardiac infarction[32,33]. We have here observed for the first time that intravenously injected MSCs remain in greater numbers for longer periods of time in emphysematous lungs in comparison with controls. There are still very low numbers of intravenously injected

http://dx.doi.org/10.4046/trd.2014.77.3.116

MSCs although MSCs had therapeutic effects on emphysema and other diseases[9]. Some researchers explain one of action mechanism that is paracrine effects by some factors such as growth factors, anti-inflammatory cytokine and immune-modulator derived from MSCs[34]. Further studies are needed on the roles of SDF-1 and the CXCR4 axis in the recruitment of stem cells to emphysematous lung and the development of COPD.

In conclusion, our results show the cellular distribution of intravenously injected MSCs shortly after injection. The specific goal of this study was to observe the cellular distribution of MSCs using appropriate tools and cross-validate these results with fluorescent and genomic findings. This is the first study to cross-validate fluorescence-labeled MSCs (i.e., the cellular level) and human-specific Alu sequences (i.e., the molecular level) and observe the cellular distribution of intravenously injected MSCs in a mouse model of emphysema. The lungs of emphysematous mice contained intravenously injected MSCs for longer periods of time in comparison with controls. These results suggest that more MSCs migrate to and remain at the injury site and Alu-based assays for quantifying transplanted MSCs are suitable for tracking the distribution of human cells in disease models.

Conflicts of Interest

No potential conflict of interest relevant to this article was reported.

Acknowledgements

The authors thank Ryeon Jin Cho for technical support, and the members of the Asan Medical Center animal facility and imaging core lab for their technical expertise. This study was supported by grants from the Korean Health Technology R&D Project, Ministry of Health & Welfare, Republic of Korea (no. HI12C0169).

References

1. Kocher AA, Schuster MD, Szabolcs MJ, Takuma S, Burkhoff D, Wang J, et al. Neovascularization of ischemic myocardium by human bone-marrow-derived angioblasts prevents cardiomyocyte apoptosis, reduces remodeling and improves cardiac function. Nat Med 2001;7:430-6.
2. Orlic D, Kajstura J, Chimenti S, Limana F, Jakoniuk I, Quaini F, et al. Mobilized bone marrow cells repair the infarcted heart, improving function and survival. Proc Natl Acad Sci U S A 2001;98:10344-9.
3. Horwitz EM, Prockop DJ, Fitzpatrick LA, Koo WW, Gordon PL, Neel M, et al. Transplantability and therapeutic effects of bone marrow-derived mesenchymal cells in children with osteogenesis imperfecta. Nat Med 1999;5:309-13.
4. Khakoo AY, Pati S, Anderson SA, Reid W, Elshal MF, Rovira II, et al. Human mesenchymal stem cells exert potent antitumorigenic effects in a model of Kaposi's sarcoma. J Exp Med 2006;203:1235-47.
5. Koc ON, Gerson SL, Cooper BW, Dyhouse SM, Haynesworth SE, Caplan AI, et al. Rapid hematopoietic recovery after coinfusion of autologous-blood stem cells and culture-expanded marrow mesenchymal stem cells in advanced breast cancer patients receiving high-dose chemotherapy. J Clin Oncol 2000;18:307-16.
6. Zhao DC, Lei JX, Chen R, Yu WH, Zhang XM, Li SN, et al. Bone marrow-derived mesenchymal stem cells protect against experimental liver fibrosis in rats. World J Gastroenterol 2005;11:3431-40.
7. Matthay MA, Goolaerts A, Howard JP, Lee JW. Mesenchymal stem cells for acute lung injury: preclinical evidence. Crit Care Med 2010;38(10 Suppl):S569-73.
8. Bonfield TL, Caplan AI. Adult mesenchymal stem cells: an innovative therapeutic for lung diseases. Discov Med 2010;9:337-45.
9. Huh JW, Kim SY, Lee JH, Lee JS, Van Ta Q, Kim M, et al. Bone marrow cells repair cigarette smoke-induced emphysema in rats. Am J Physiol Lung Cell Mol Physiol 2011;301:L255-66.
10. Longhini-Dos-Santos N, Barbosa-de-Oliveira VA, Kozma RH, Faria CA, Stessuk T, Frei F, et al. Cell therapy with bone marrow mononuclear cells in elastase-induced pulmonary emphysema. Stem Cell Rev 2013;9:210-8.
11. Cruz FF, Antunes MA, Abreu SC, Fujisaki LC, Silva JD, Xisto DG, et al. Protective effects of bone marrow mononuclear cell therapy on lung and heart in an elastase-induced emphysema model. Respir Physiol Neurobiol 2012;182:26-36.
12. Shigemura N, Okumura M, Mizuno S, Imanishi Y, Nakamura T, Sawa Y. Autologous transplantation of adipose tissue-derived stromal cells ameliorates pulmonary emphysema. Am J Transplant 2006;6:2592-600.
13. Katsha AM, Ohkouchi S, Xin H, Kanehira M, Sun R, Nukiwa T, et al. Paracrine factors of multipotent stromal cells ameliorate lung injury in an elastase-induced emphysema model. Mol Ther 2011;19:196-203.
14. Schweitzer KS, Johnstone BH, Garrison J, Rush NI, Cooper S, Traktuev DO, et al. Adipose stem cell treatment in mice attenuates lung and systemic injury induced by cigarette smoking. Am J Respir Crit Care Med 2011;183:215-25.
15. Gupta N, Su X, Popov B, Lee JW, Serikov V, Matthay MA. Intrapulmonary delivery of bone marrow-derived mesenchymal stem cells improves survival and attenuates endotoxin-induced acute lung injury in mice. J Immunol 2007;179:1855-63.
16. Aslam M, Baveja R, Liang OD, Fernandez-Gonzalez A, Lee C, Mitsialis SA, et al. Bone marrow stromal cells attenuate lung

injury in a murine model of neonatal chronic lung disease. Am J Respir Crit Care Med 2009;180:1122-30.
17. Yukawa H, Kagami Y, Watanabe M, Oishi K, Miyamoto Y, Okamoto Y, et al. Quantum dots labeling using octa-arginine peptides for imaging of adipose tissue-derived stem cells. Biomaterials 2010;31:4094-103.
18. Yukawa H, Watanabe M, Kaji N, Okamoto Y, Tokeshi M, Miyamoto Y, et al. Monitoring transplanted adipose tissue-derived stem cells combined with heparin in the liver by fluorescence imaging using quantum dots. Biomaterials 2012;33:2177-86.
19. Mighell AJ, Markham AF, Robinson PA. Alu sequences. FEBS Lett 1997;417:1-5.
20. Schmid CW. Alu: structure, origin, evolution, significance and function of one-tenth of human DNA. Prog Nucleic Acid Res Mol Biol 1996;53:283-319.
21. Nicklas JA, Buel E. Development of an Alu-based, real-time PCR method for quantitation of human DNA in forensic samples. J Forensic Sci 2003;48:936-44.
22. Nicklas JA, Buel E. Development of an Alu-based, QSY 7-labeled primer PCR method for quantitation of human DNA in forensic samples. J Forensic Sci 2003;48:282-91.
23. Kim SY, Lee JH, Kim HJ, Park MK, Huh JW, Ro JY, et al. Mesenchymal stem cell-conditioned media recovers lung fibroblasts from cigarette smoke-induced damage. Am J Physiol Lung Cell Mol Physiol 2012;302:L891-908.
24. Kraitchman DL, Tatsumi M, Gilson WD, Ishimori T, Kedziorek D, Walczak P, et al. Dynamic imaging of allogeneic mesenchymal stem cells trafficking to myocardial infarction. Circulation 2005;112:1451-61.
25. Li Q, Zhou X, Shi Y, Li J, Zheng L, Cui L, et al. *In vivo* tracking and comparison of the therapeutic effects of MSCs and HSCs for liver injury. PLoS One 2013;8:e62363.
26. Lin S, Xie X, Patel MR, Yang YH, Li Z, Cao F, et al. Quantum dot imaging for embryonic stem cells. BMC Biotechnol 2007;7:67.
27. Garrovo C, Bergamin N, Bates D, Cesselli D, Beltrami AP, Lorenzon A, et al. In vivo tracking of murine adipose tissue-derived multipotent adult stem cells and *ex vivo* cross-validation. Int J Mol Imaging 2013;2013:426961.
28. Harting MT, Jimenez F, Xue H, Fischer UM, Baumgartner J, Dash PK, et al. Intravenous mesenchymal stem cell therapy for traumatic brain injury. J Neurosurg 2009;110:1189-97.
29. Son BR, Marquez-Curtis LA, Kucia M, Wysoczynski M, Turner AR, Ratajczak J, et al. Migration of bone marrow and cord blood mesenchymal stem cells *in vitro* is regulated by stromal-derived factor-1-CXCR4 and hepatocyte growth factor-c-met axes and involves matrix metalloproteinases. Stem Cells 2006;24:1254-64.
30. Chen T, Bai H, Shao Y, Arzigian M, Janzen V, Attar E, et al. Stromal cell-derived factor-1/CXCR4 signaling modifies the capillary-like organization of human embryonic stem cell-derived endothelium *in vitro*. Stem Cells 2007;25:392-401.
31. Zhang Y, Wittner M, Bouamar H, Jarrier P, Vainchenker W, Louache F. Identification of CXCR4 as a new nitric oxide-regulated gene in human CD34+ cells. Stem Cells 2007;25:211-9.
32. Werner L, Guzner-Gur H, Dotan I. Involvement of CXCR4/CXCR7/CXCL12 Interactions in Inflammatory bowel disease. Theranostics 2013;3:40-6.
33. Theiss HD, Vallaster M, Rischpler C, Krieg L, Zaruba MM, Brunner S, et al. Dual stem cell therapy after myocardial infarction acts specifically by enhanced homing via the SDF-1/CXCR4 axis. Stem Cell Res 2011;7:244-55.
34. Murphy MB, Moncivais K, Caplan AI. Mesenchymal stem cells: environmentally responsive therapeutics for regenerative medicine. Exp Mol Med 2013;45:e54.